

Iridium(I) Complexes of Upper Rim Functionalized PTA Derivatives. Synthesis, Characterization, and Use in Catalytic Hydrogenations (PTA = 1,3,5-Triaza-7-phosphaadamantane)

Antonella Guerriero,[†] Mikael Erlandsson,[†] Andrea Ienco,[†] Donald A. Krogstad,[‡] Maurizio Peruzzini,^{*,†} Gianna Reginato,[†] and Luca Gonsalvi^{*,†}

[†]Consiglio Nazionale delle Ricerche, Istituto di Chimica dei Composti Organometallici (ICCOM-CNR), Via Madonna del Piano 10, 50019 Sesto Fiorentino (Firenze), Italy

[‡]Concordia College at Moorhead, 334F Ivers, Moorhead, Minnesota 56562, United States

S Supporting Information

ABSTRACT: Reaction of (1,3,5-triaza-7-phosphaadamantane-6-yl)lithium (**1**; PTA-Li), synthesized in high yield and purity, with *p*-(dimethylamino)benzaldehyde gave the novel water-soluble β -phosphino alcohol (4'-(dimethylamino)phenyl) (1,3,5-triaza-7-phosphatricyclo[3.3.1.1]dec-6-yl)methanol (**2**; PZA-NMe₂). The oxide O=PZA-NMe₂ (**3**) and sulfide S=PZA-NMe₂ (**4**) were also obtained. Ir(I) complexes of (*S,R,S*)-PZA-NMe₂ and the analogue phenyl(1,3,5-triaza-7-phosphatricyclo[3.3.1.1]dec-6-yl)methanol (PZA) were obtained and used as precatalysts for the hydrogenation of α,β -unsaturated aldehydes and ketones and acetophenone using different mild reduction protocols. The X-ray crystal structure of the *S,R,S* diastereoisomer of PZA-NMe₂ was also obtained and is described herein.

1. INTRODUCTION

The increasing need to replace old technologies with sustainable approaches,¹ including minimization of large quantities of organic solvents and waste, has prompted a renewed interest in the search for alternative media for chemical transformations. In particular, the use of water as an alternative solvent has witnessed a true renaissance in the past few years, often in homogeneous transition-metal-catalyzed processes.² The first issue to be addressed in the quest for a water-soluble homogeneous catalyst is to design a versatile structure able to convey the electronic and steric properties of known active organometallic complexes into water. The resulting precatalyst, and corresponding activated species, must therefore be stable in water in order to bring about the desired catalytic transformation with high activities and selectivities. This would allow for its recycling and reuse by simple phase separation in the case of biphasic water/organic solvent media.

All these issues have been addressed by many research groups, each proposing different ways to obtain water-soluble catalysts.³ The most common approach is to modify known ligands, such as (bidentate) phosphines and amines, amino alcohols, and their combinations, by introducing polar charged groups, i.e. SO₃⁻, NR₃⁺, CO₂⁻, and phosphonates.^{2c} This in turn increases the water solubility due to solvation and separate ion couple formation.

In spite of the great amount of literature data published, a class of ligands having a molecular scaffold which is conceptually simple, versatile in its coordination to transition metals, and easy to handle and to functionalize, for example by introducing other

binding groups and/or chiral centers, has not yet been fully identified and developed.

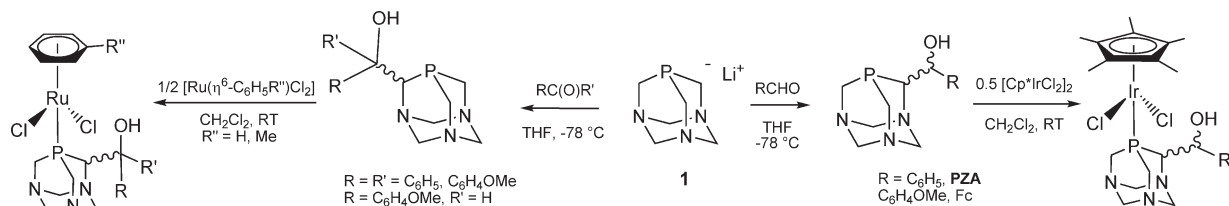
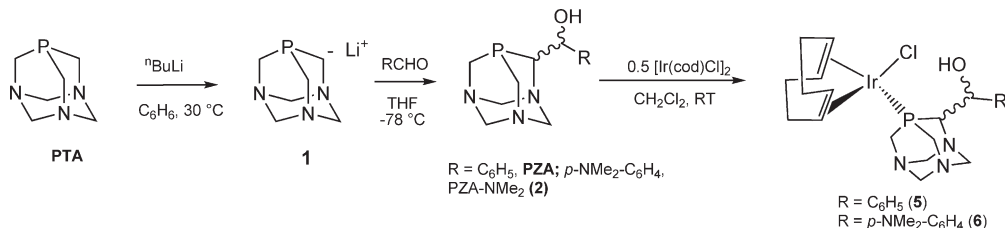
During the past few years, there has been a renewed interest in the use of the neutral water-soluble cage monodentate phosphine PTA (PTA = 1,3,5-triaza-7-phosphaadamantane)⁴ and its structural modifications.⁵ A large number of coordination compounds have been synthesized, and their catalytic,⁶ medicinal,⁷ and electrochemical properties⁸ have been investigated, together with mechanistic aspects of Ru-PTA mediated hydrogen activation in water.⁹ The easiest way to modify PTA is to alkylate phosphorus or nitrogen atoms^{10,11} or to open the cage, giving potentially bidentate P,N¹² or tridentate P,N,N¹³ derivatives. More recently, the bidentate phosphine PTA-PPh₂, containing a binding side arm and a chiral center on the C_α to P, was obtained by Frost and co-workers by reaction of PTA with ⁿBuLi and ClPPh₂.¹⁴ The key intermediate, (1,3,5-triaza-7-phosphaadamantane-6-yl)lithium (**1**; PTA-Li), was isolated as a highly pyrophoric compound, and the subsequent reaction with the chlorophosphine was carried out in a DME slurry at room temperature, resulting in only a 10% yield of the final compound after workup (Scheme 1).

Later on, the Frost group¹⁵ and our laboratory¹⁶ independently reported on the reaction of **1** with aryl aldehydes^{15,16} and ketones,¹⁵ yielding a series of water-soluble β -phosphino alcohols (PTA-CRR'OH: R = C₆H₅, C₆H₄OCH₃, ferrocenyl; R' = H, C₆H₅, C₆H₄OCH₃). Some ligands were used to coordinate

Received: November 29, 2010

Published: March 09, 2011

Scheme 1. Synthesis and Coordination Properties of PTA Upper Rim Derivatives

Scheme 2. Synthesis of PTA-Li (1), PZA, and PZA-NMe₂ (2) and Their Ir(I) Complexes

Ru(II) arene moieties,¹⁵ whereas phenyl(1,3,5-triaza-7-phosphatricyclo[3.3.1.1]dec-6-yl)methanol (PZA) was used to bind the Ir(III) pentamethylcyclopentadienyl core.¹⁶ In all cases a $\kappa^1\text{P}\eta^1$ binding mode was observed, as shown in Scheme 1.

Herein, we describe an improved method for the synthesis of **1** and new derivatives of PTA upper rim functionalization, namely the novel phosphino alcohol (4'-(dimethylamino)phenyl)(1,3,5-triaza-7-phosphatricyclo[3.3.1.1]dec-6-yl)methanol, (**2**; PZA-NMe₂) and its oxide O=PZA-NMe₂ (**3**) and sulfide S=PZA-NMe₂ (**4**) together with Ir(I) complexes of PZA and PZA-NMe₂. The latter were used as precatalysts for catalytic hydrogenations of model substrates including linear α,β -unsaturated aldehydes and ketones, namely cinnamaldehyde (CNA) and benzylideneacetone (BZA), and cyclic species such as 2-cyclohexen-1-one and simple aryl alkyl ketones (acetophenone). Different reduction protocols were employed, specifically transfer hydrogenation (TH) in the presence of either HCO₂Na/H₂O or KOH/^{*i*}PrOH or in a combined hydrogenation/transfer hydrogenation protocol (H₂ 30 bar/^{*t*}BuOK/^{*i*}PrOH) run at room temperature.¹⁷

2. RESULTS AND DISCUSSION

2.1. Synthesis and Characterization of PTA Derivatives.

Following our initial interest in PTA structural modifications, we considered the use of (1,3,5-triaza-7-phosphatricyclo[3.3.1.1]dec-6-yl)lithium (**1**; PTA-Li) as a valuable intermediate to obtain multidentate, water-soluble, enantiomerically enriched ligands for transition-metal complexes. In order to improve on the yields and purity of **1** and, in turn, of the ligands derived by its reaction with electrophiles, we introduced slight but important changes in the synthetic protocol¹⁴ originally comprising the reaction of PTA with ^{*n*}BuLi in THF at -78°C . Due to the limited solubility of PTA under such conditions, the reaction suffered from the main disadvantages of being carried out under heterogeneous conditions and cumbersome workup being needed to separate the products from omnipresent PTA after quenching with water. We found that when the lithiation reaction was carried out in warm benzene (ca. 30°C), PTA was completely soluble under such conditions, and the lithium derivative **1** precipitated out of

the reaction mixture as an analytically pure microcrystalline powder after addition of ^{*n*}BuLi (Scheme 2). The solid can be therefore recovered by filtration under nitrogen and stored for subsequent use. We noted that, although all efforts were made to exclude moisture from the Schlenk tubes used for storage, the batch should be used within 1 week to ensure the highest purity of the reagent.

Subsequent reaction of **1** with electrophiles such as benzaldehyde was carried out as previously described: i.e., by addition of the aldehyde to a suspension of **1** in THF at -78°C , followed by quenching with ice-cold water. This afforded PZA as a mixture of two diastereoisomers having comparable solubility properties in water and other common organic solvents, as shown by solubility tests and ³¹P{¹H} spectra (D₂O, two singlets at -103.4 and -106.6 ppm, 1:1 ratio).¹⁶

We have previously shown¹⁶ in the case of the oxide O=PZA that solubility can be pivotal to diastereoisomer separation by simple crystallization from suitable solvent mixtures. For this compound, the P=O oxygen atom forms a strong intermolecular hydrogen bond with the hydroxyl group of a neighboring PZA-(O) molecule (O...OH distance 2.717(6) Å), giving a mono-dimensional infinite chain in the solid state. This could account for the poor solubility of the *SR,RS* diastereoisomer. Thus, we reasoned that subtle changes in the PZA framework by introduction of substituents on the phenyl ring could in principle modify the hydrogen-bonding network and henceforth change the solubility properties of the two diastereoisomers, without significantly affecting the donor properties of the P atom of the cage.

Therefore, the new moderately water-soluble (S(H₂O)₂₀)₂₀ = 1.9 g/L) phosphino alcohol ligand (4'-(dimethylamino)phenyl)(1,3,5-triaza-7-phosphatricyclo[3.3.1.1]dec-6-yl)methanol (**2**; PZA-NMe₂) was synthesized by replacing benzaldehyde with 4-(dimethylamino)benzaldehyde. ³¹P{¹H} NMR spectra of the crude reaction mixture in CDCl₃ showed the presence of two singlets in a 3:1 ratio at -102.72 (major, **2a**) and -106.27 (minor, **2b**). As expected, the major diastereoisomer **2a** was isolated after fractional crystallization and characterized by single-crystal X-ray diffraction, showing that **2a** corresponds to the *SR,RS* diastereoisomer (see section 2.2).

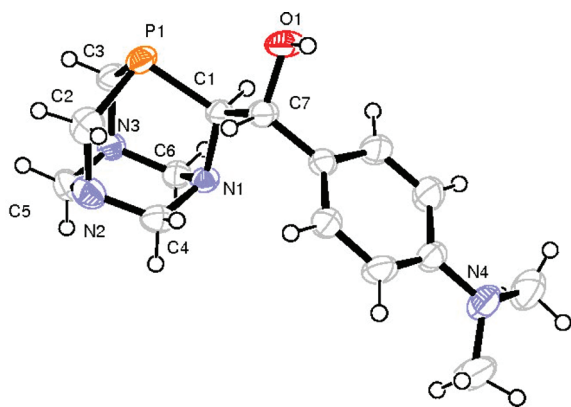


Figure 1. ORTEP view of **2a**. Ellipsoids are drawn at the 50% probability level. Selected bond lengths (Å) and angles (deg) for **2a**: P1–C1 = 1.8695(16); P1–C2 = 1.859(2); P1–C3 = 1.8503(19); C1–N1 = 1.476(2); C2–N2 = 1.476(3); C3–N3 = 1.470(2); C7–O1 = 1.420(2); C1–C7 = 1.531(2); C7–C1–P1 = 111.62(11); N1–C1–C7 = 112.86(13).

In solution, the loss of symmetry of the PTA cage upon functionalization of the 6-position was evident from the magnetic inequivalence of the methylene protons in the ^1H NMR spectrum of **2a**, with an AB multiplet centered at 4.85 ppm ($^2J_{\text{H}_a, \text{H}_b} = 13.4$ Hz) and a multiplet in the range 4.57–4.37 ppm corresponding to the remaining four NCH_2N protons. A similar situation was observed for the upper rim protons appearing as three overlapped groups of signals between 4.29 and 3.80 ppm. In keeping with the loss of the adamantane symmetry, the $^{13}\text{C}\{^1\text{H}\}$ NMR spectrum of **2a** showed two signals at 74.20 and 67.78 ppm for the NCH_2N carbon atoms and three doublets at 65.75 (PCHN) and 51.55 and 48.43 ppm (PCH₂N) with $^1J_{\text{CP}}$ values ranging from 19.9 to 24.0 Hz.

The main problem encountered in the syntheses of PZA and PZA-NMe₂ was the tedious workup, involving column chromatography. This dramatically decreased the overall yields but was needed to obtain analytically pure compounds. This procedure was indeed mandatory for the following use as ligands toward Ir(I) precursors, particularly in the case of PZA (see section 2.3).

The syntheses of O=PZA-NMe₂ (**3**) and S=PZA-NMe₂ (**4**) were carried out straightforwardly by reacting **2a** with either aqueous H₂O₂ at room temperature or S₈ under reflux conditions. Selective protection (oxidation) of the P atom was achieved in both cases, as evidenced by the presence of a singlet in the $^{31}\text{P}\{^1\text{H}\}$ NMR spectra of the reaction mixtures, at 2.09 and –14.07 ppm, respectively, at values expected from comparison with the spectra for PTA⁴ and PZA.¹⁶

2.2. X-ray Crystal Structure of (SR,RS)-(4'-(Dimethylamino)phenyl)(1,3,5-triaza-7-phosphatricyclo[3.3.1.1]dec-6-yl)methanol (2a). The X-ray structure of **2a** contains both SR and RS enantiomers in the unit cell. Figure 1 give an ORTEP drawing with selected distances and angles in the caption. As previously noted for other upper rim PTA compounds,^{15,16} the P1–C1 bond (1.8695(16) Å) is slightly longer than the other two P–C bonds (P1–C2 = 1.859(2) Å, P1–C3 = 1.8503(19) Å), while the C–N bonds of the adamantane cage do not differ significantly.

The hydroxyl group forms a strong intramolecular hydrogen bond with a nitrogen atom of a neighboring molecule (O1···N3#1 = 2.7821(19) Å, where the symmetry transformation used to generate the equivalent atom is $x, -1 + y, z$). A 1D infinite chain can be recognized along the b axis, as shown in

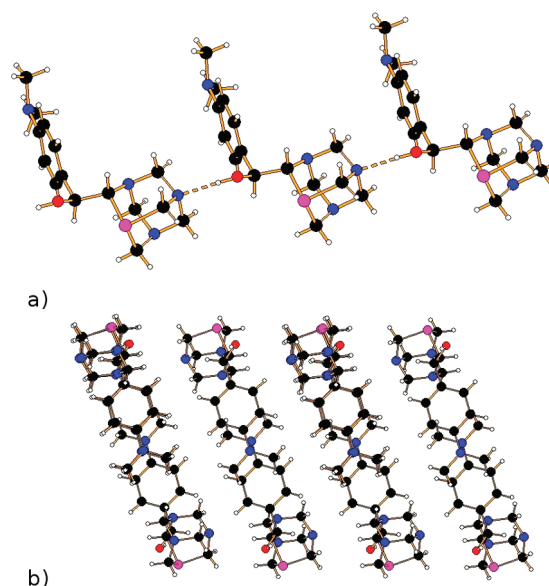


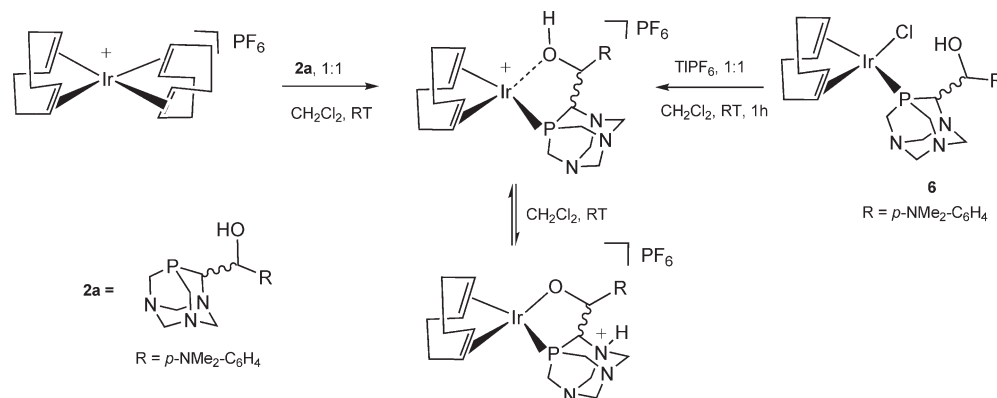
Figure 2. (a) Intermolecular OH···N hydrogen bonding in **2a**, with a view along the a axis. (b) Packing within the asymmetric unit, with a view along the b axis parallel to hydrogen bonds.

Figure 2a. The π ··· π stacking of the (dimethylamino)phenyl groups holds together two of the 1D chains. The latter supramolecular units arrange themselves in the space, as seen from the packing diagram (Figure 2b) along the b axis. The existence of a hydrogen bond 1D chain was also found in O=PZA-CH(C₆H₄OCH₃)OH¹⁵ and O=PZA-CH(C₆H₅)OH (O=PZA),¹⁶ while two O=PZA-C(C₆H₄OCH₃)₂OH and four PTA-C(C₆H₄OCH₃)₂OH units form a hydrogen bonded dimer and tetramer, respectively. Interestingly, while the intermolecular hydrogen-bonding network is established between the P=O oxygen and the hydroxyl group of a neighboring O=PZA molecule, for **2a** this occurs by connecting the hydroxyl OH group with a N atom of the adamantane cage.

2.3. Synthesis and Characterization of Ir(I) Complexes of PZA and PZA-NMe₂. The coordination chemistry of PTA and its derivatives with Ir has been far less investigated than for other late transition metals relevant to homogeneous catalysis such as Ru, Rh, and Pd.⁵ To date, only one Ir(0),¹⁸ four Ir(I),^{6f,19} and six Ir(III) PTA^{16,20} complexes have been reported, and some of these last six were used as catalysts for the hydrogenation of bicarbonate to formate.²¹

On the basis of the limited amount of Ir complexes of PTA and derivatives in the literature and in view of the possible applications of such compounds as catalysts for reactions in water phase or biphasic water/organic solvent,²² we thought it timely to explore the coordination chemistry of PZA and (SR,RS)-PZA-NMe₂ with Ir(I). Both ligands were therefore reacted in a 2:1 ratio with the dimeric precursor [Ir(cod)Cl]₂ in either CH₂Cl₂ or CH₂Cl₂/toluene at room temperature, to obtain the complexes [Ir(cod)Cl(PZA)] (**5**) and [Ir(cod)Cl{(SR,RS)-(PZA-NMe₂)}] (**6**) in moderate to good yields after simple workup (Scheme 2).

Whereas the racemic mixture containing **2a** as a single diastereoisomer was used to synthesize **6**, complex **5** was obtained as a racemic mixture of four enantiomers containing both diastereoisomers present in PZA. Since all our attempts to grow suitable crystals to determine the solid-state structure of **5** and **6** had failed thus far, the proposed formulas were demonstrated by elemental

Scheme 3. Proposed Mechanism for the Switch from a $\kappa^1\text{P}$ to a $\kappa^2\text{P,O}$ Coordination Mode in **6**

analysis and solution NMR and ESI-MS data. Complex **6** exhibited a singlet at -64.09 ppm in the $^{31}\text{P}\{^1\text{H}\}$ NMR spectrum (one diastereoisomer), while the ^1H NMR signals corresponding to the η^4 -coordinated cyclooctadiene were partially overlapping the PCH_2N methylene signals and were partially identifiable in the range 2.25–1.68. The $^{13}\text{C}\{^1\text{H}\}$ NMR data are more diagnostic for this ligand, in particular the CH signals at 98.07 (d, $^2J_{\text{CP}} = 12.8$ Hz) and 97.13 (d, $^2J_{\text{CP}} = 13.7$ Hz), again reflecting the lack of symmetry in the molecule. The NMR characterization is slightly more complicated for **5**, due to the presence of two diastereoisomers giving $^{31}\text{P}\{^1\text{H}\}$ NMR singlets at -64.97 and -58.50 ppm, but is substantially similar to the case for **6**. The C, H, N elemental analysis and ESI-MS data (m/z 564.2 $[\text{Ir}(\text{cod})(\text{PZA})]^+$, 605.3 $[\text{Ir}(\text{cod})(\text{PZA-NMe}_2)]^+$) confirm the presence of (labile) chloride ligand and support the proposed formulas. Conductivity data were obtained for **6** in various solvents. As expected, in CH_2Cl_2 the complex was not substantially conductive in nature, whereas partial chloride dissociation may be possible in polar solvents such as MeOH and H_2O , however, giving low conductivity values (0.032 and 0.064 mS/cm, respectively).

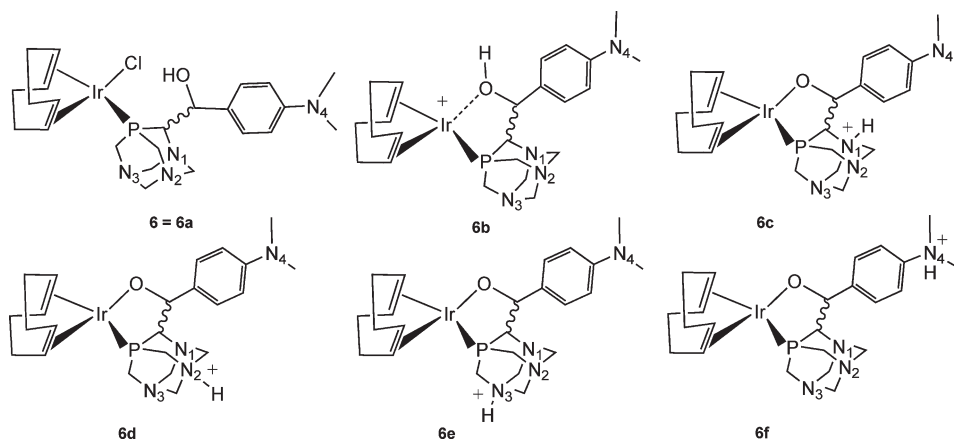
The lability of the chloride ligand in polar solvents and the presence of phosphorus and oxygen donor atoms on PZA and PZA-NMe₂ could, in principle, favor the formation of $\kappa^2\text{P,O}$ chelate analogues of **5** and **6** in solution. In order to verify this possibility, complex **6** was reacted with a chloride scavenger (TIPF₆) in CH_2Cl_2 at room temperature. The initial yellow solution immediately turned red. After 1 h of stirring, TiCl was removed by filtration and an aliquot of the solution was analyzed by $^{31}\text{P}\{^1\text{H}\}$ NMR, showing a singlet at -17.04 ppm and a septet at ca. -146 ppm (PF₆). The low-field NMR shift from -64.1 ppm due to **6** to -17.04 ppm can be attributed to both the formation of a cationic species such as $[\text{Ir}(\text{cod})(\text{PZA-NMe}_2)]^+$ and the Δ -ring contribution upon $\kappa^2\text{P,O}$ coordination.²³ To further validate this hypothesis, **2a** was reacted in a 1:1 ratio with the Ir(I) precursor $[\text{Ir}(\text{cod})_2]\text{PF}_6$ in CH_2Cl_2 at room temperature. After 2 h of stirring, the $^{31}\text{P}\{^1\text{H}\}$ NMR spectrum confirmed the presence of the singlet at -17.04 ppm. Interestingly, when the solution was left standing for 24 h, the singlet at -17.04 ppm decreased in intensity and a new signal at -53.4 ppm appeared, for a final 1:5 ratio between the two species on the basis of NMR data.²⁴ In the absence of coordinating solvents which could stabilize $\kappa^1\text{P}$ cationic derivatives, equilibria involving different $\kappa^2\text{P,O}$ species may be active. In particular, due to the relative acidity of the OH proton and the basicity of the N atoms in the triazacyclohexane bottom rim on the PTA skeleton, a

protonation–deprotonation intermolecular equilibrium could be possible in this case (Scheme 3).

DFT theoretical calculations were used to verify the possible replacement of Cl with an OH group on the ligand for **5** and **6** and the energies associated with a protonation–deprotonation intermolecular equilibrium. The effects of the substituent of the phenyl group on the geometrical parameters was found to be relatively small, and for sake of conciseness only the results relevant to **6** are discussed here. Several models were considered. In particular the structures related to **6a**, a model of **6** with $\kappa^1\text{P}$ coordination mode of PZA-NMe₂ and **6b**, having a $\kappa^2\text{P,O}$ bonding mode of the ligand, were optimized in the gas phase. Regarding the intermolecular equilibrium, there are in principle four nitrogen atoms (N1–N4, Scheme 4) that could act as proton acceptors for the hydroxyl deprotonation and consequently four models (**6c–f**) should be considered. On a closer look (Scheme 4), two of them (**6d,e**), namely with protonation at the N2 and N3 nitrogen atoms, are equivalent; thus, only **6d** was optimized. Moreover, in the discussion of the structures only **6c** is considered, as the main geometrical features of the optimized species **6c,d,f** were found to be quite similar.

In the conformers **6a–c**, reported in Figure 3, the Ir atoms have a square-planar coordination environment. The Ir–C distances *trans* to the phosphine ligand are slightly longer than those *trans* to chlorine or oxygen atoms (average 2.21 Å vs 2.13 Å and 2.26 Å vs 2.14 Å for **6a,b**, respectively) while the C=C bonds *trans* to P (1.40 Å) are shorter than those *trans* to Cl and O atoms (1.43 Å) in all the optimized models. The metal back-donation is more effective for the C=C bonds *trans* to O and Cl atoms, but the substitution of the oxygen atom with chlorine did not have an influence on C=C distances. The Ir–P distance is calculated at 2.31 Å in **6b** (2.33 Å for **6c**), while it was 2.35 Å in **6a**. The shortening of the M–P distance is a consequence of the ring-closing strain. The latter effect can also be measured by comparing the Cl–Ir–P (90.1°) and O–Ir–P (78.4 and 81.5° for **6b,c**) angles and the Ir–P–Cl angles (114.5, 102.7, and 98.6° for **6a–c**, respectively).

Compounds **6b–f** were examined in an effort to identify the most likely protonated species of the intermolecular equilibrium. The energy differences calculated in CH_2Cl_2 solution show that **6c** is more stable (3.7 kcal mol⁻¹) relative to **6f**, which is expected considering amines substituted by aromatics have basicities lower than those substituted by alkyl groups. It is also noteworthy that the energy difference between **6c** and **6d** is 3.8 kcal mol⁻¹. The latter value has to be compared with the difference ($\Delta G = 0.1$ kcal mol⁻¹)

Scheme 4. Possible Structures 6a–f Deriving from Protonation and $\kappa^1\text{P}$ to $\kappa^2\text{P,O}$ Coordination Switch in 6

between the N1 and N2 protonated species. Finally, the hydroxyl **6b** complex is more stable than **6c** ($2.9 \text{ kcal mol}^{-1}$). These results support the hypothesis of the possible presence of an N-protonated zwitterionic complex (**6c**) and also discriminate between the nitrogen atoms of the ligand as the preferred protonation site.

2.4. Catalytic Hydrogenations of Aldehydes and Ketones under Mild Conditions. Few examples of catalytic applications of Ir complexes bearing PTA or derivatives as ancillary ligands can be found in the literature. The iridium compounds $[\text{Ir}(\text{cod})(\text{PTA})_3]\text{Cl}$, $[\text{IrCl}(\text{CO})(\text{PTA})_3]$, and $[\text{Ir}(\text{CO})(\text{PTA})_4]\text{Cl}$ were found to be active for the cyclization of 4-pentyn-1-amine to 2-methylpyrroline in water at 50°C .^{6f} $[\text{Cp}^*\text{IrCl}(\text{PTA})_2]\text{Cl}$ was tested as a catalyst for $\text{CO}_2/\text{HCO}_3^-$ reduction to formate, in the absence of base additive and under mild conditions, in the pH range 5.3–10.5 and in the temperature range $30\text{--}100^\circ\text{C}$. The complex showed good activity at elevated temperatures and in slightly basic aqueous solution (pH 9), forming the corresponding cationic $[\text{Cp}^*\text{IrH}(\text{PTA})_2]^+$ complex as the catalytically active species.²¹

Ir-catalyzed chemo- and enantioselective hydrogenations²⁵ and transfer hydrogenations²⁶ of compounds of industrial interest such as alkenes, ketones, aldehydes, and α,β -unsaturated carbonyl compounds in water or biphasic systems are known, using bidentate ligands such as 4,4'-dihydroxy-2,2'-bipyridine,²⁷ Noyori's (*R,R*)-TsDPEN and derivatives, ((*R,R*)-TsDPEN = (1*R*,2*R*)-*N*-(*p*-toluenesulfonyl)-1,2-diphenylethylenediamine),²⁸ (1*S*,2*R*)-(+)-norephedrine and (1*R*,2*S*)-(–)-ephedrine,²⁹ and other systems such as $[\text{Ir}(\text{cod})\text{Cl}]_2$ in combination with HSA (HSA = human serum albumin),³⁰ to name just a few. No Ir-PTA complexes have so far been reported to perform these transformations. More attention has been paid to Ru and Rh compounds such as *cis*- $\text{RuCl}_2(\text{PTA})_4$,³¹ *trans*- $[\text{Ru}_4(\text{mPTA})_2]$, $[\text{Ru}_2(\text{mPTA})_3(\text{H}_2\text{O})]\text{I}_3$, and $[\text{Rh}_4(\text{mPTA})_2]\text{I}$ (mPTA = *N*-methyl-PTA),³² and half-sandwich Ru-PTA complexes bearing ancillary ligands such as Cp, Cp*,³³ Dp, and Ind (Cp = η^5 -cyclopentadienyl; Cp* = η^5 -pentamethylcyclopentadienyl; Dp = η^4 -dihydrocyclopentadienyl; Ind = η^5 -indenyl),^{6a,34} which were observed to promote catalytic hydrogenations of alkenes, unsaturated aldehydes, ketones and other substrates under either transfer hydrogenation or hydrogen pressure in water or biphasic systems.⁵ In all cases, although promising, these water-phase systems rarely match the performance obtained by the most efficient Ru-based catalysts showing very high turnover frequencies (TOFs).³⁵ The need is

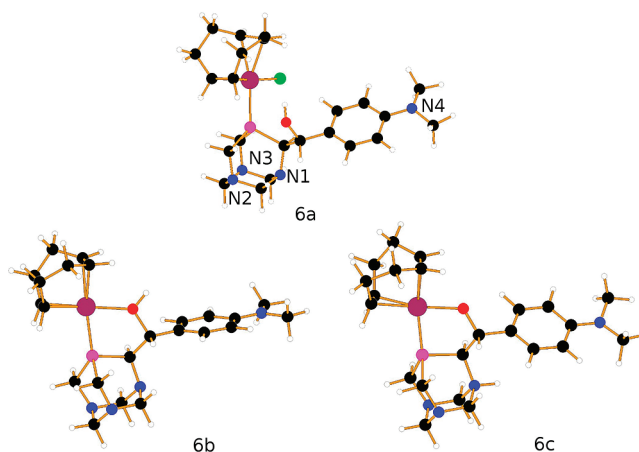


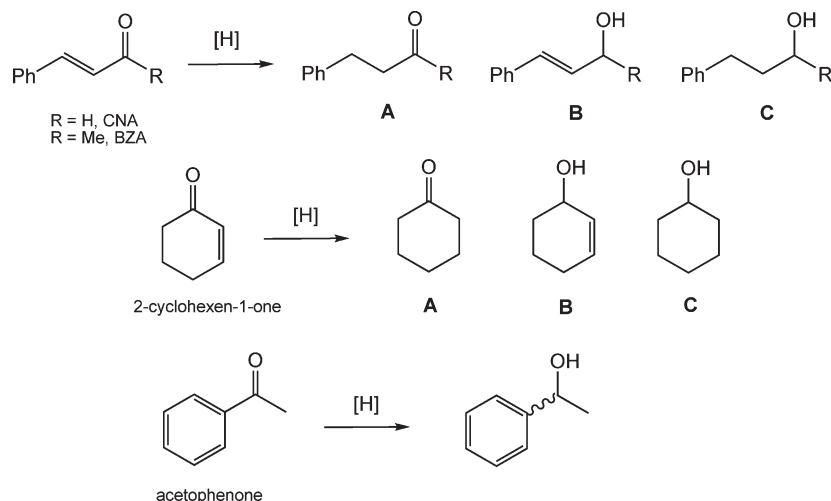
Figure 3. Optimized structures for the isomers $\kappa^1\text{P}$ (**6a**), $\kappa^2\text{P,OH}$ (**6b**) and $\kappa^2\text{P,O}$ (**6c**). Color code: oxygen, red; nitrogen, blue; phosphorus, pink; chlorine, green; iridium, purple (large sphere); carbon, black (small sphere); hydrogen, white.

indeed for mild protocols which can be applied using water as solvent and the tolerance to different functional groups, resulting in high chemoselectivities.²

We tested complexes **5** and **6** as catalysts for the chemoselective hydrogenation of model substrates including linear α,β -unsaturated aldehydes and ketones (CNA, BZA), cyclic species (2-cyclohexen-1-one), and simple aryl alkyl ketones (acetophenone) using different reduction protocols (Scheme 5).³⁶

Sodium formate is one of the mildest reducing agents and affords a wide compatibility between functional groups and water solubility. In order to ensure complete solubility of all reagents and formation of a homogeneous phase at moderate temperatures, it is often required to add a variable percentage of an organic solvent, usually an alcohol. Thus, transfer hydrogenation (TH) of CNA using HCO_2Na was carried out in water/methanol at different temperatures and variable catalyst/CNA ratios.

A black precipitate, likely bulk metal, was observed upon running the tests at 80 and 60°C , suggesting that the complexes were not stable under the conditions applied. This assumption was supported by the fact that phosphine oxide **3** was the only P-containing species observed by ^{31}P NMR analysis of an aliquot of the reaction mixture. The conversions observed at 6 h, 80°C

Scheme 5. Hydrogenation Test Reactions Involving α,β -Unsaturated Aldehydes, Ketones, and AcetophenoneTable 1. Transfer Hydrogenation of CNA with **5** and **6** using $\text{HCO}_2\text{Na}/\text{H}_2\text{O}/\text{MeOH}$

entry	precat.	solvent ratio MeOH/H ₂ O	conversion (%) (time (h))	yield (%)			TON (av)
				A ^b	B ^b	C ^b	
1	5 ^a	1/2	99.4 (8)	0.7	77.6	21.1	99
2	5 ^{a,c}	1/2	68.5 (8)	4.5	47.2	16.8	69
3	6 ^a	1/1	96.6 (6)	3.1	78.0	15.5	97
4	6 ^a	1/1	99.3 (24)	0.6	79.0	19.7	99
5	6 ^{a,c}	1/1	57.4 (6)	9.7	43.2	4.5	57
6	6 ^{a,c}	1/1	78.7 (24)	7.3	61.9	9.5	79

^a Conditions: CNA, 0.75 mmol; catalyst, 7.5×10^{-3} mmol; HCO_2Na , 7.5 mmol; total volume of solvents, 6 mL; 40 °C. ^b GC values based on pure samples: A = hydrocinnamaldehyde; B = cinnamol; C = 3-phenyl-1-propanol. ^c One drop of Hg(0) added.

(99.1%, **5**; 83.3%, **6**), yielding a ca. 2:1 mixture of cinnamol and 3-phenyl-1-propanol, could be therefore due to the formation of unperceived phosphine oxide stabilized metal nanoparticles or soluble metal colloids.³⁷ The runs were repeated at 40 °C in order to test the effect of temperature on the stability of the catalyst and its performance under milder conditions. In parallel, Hg(0) poisoning tests were carried out under the same conditions to establish whether a significant amount of heterogeneously catalyzed reactions were responsible for the results observed.³⁸

The results are summarized in Table 1. It can be seen that, although cinnamol is always the favored product, a significant decrease in activity and selectivity is observed in the Hg-poisoning tests for both catalysts, thus confirming that a mixed heterogeneous/homogeneous system is active under these conditions. The tests were also run at higher catalyst/substrate ratios (1/500 and 1/1000, respectively), but in this case the competing base-catalyzed aldol condensation reaction dominates, yielding significant amounts of dimerization side products, identified by GC-MS analysis.

Transfer hydrogenation of BZA using HCO_2Na in water/methanol at 60 °C in the presence of **6** (1/100 catalyst to substrate ratio) showed that the reaction gave a maximum conversion of ca. 55% at 24 h and a ca. 4:1 ratio between saturated ketone and unsaturated alcohol (Table 2, entries 1 and 2).

For the reduction of 2-cyclohexen-1-one, both the $\text{HCO}_2\text{Na}/\text{H}_2\text{O}/\text{MeOH}$ protocol (Table 2, entries 3 and 4) and the more

commonly used $\text{KOH}/i\text{PrOH}$ method (Table 2, entries 7 and 8) were applied in the presence of **6**, using catalyst/substrate ratios of 1/100 and 1/500, respectively. In the first case, hydrogenation was selective for cyclohexanone, with a maximum conversion of 67% after 24 h. In contrast, after 24 h at 80 °C the stronger reducing agent KOH brings about the reduction to cyclohexanol (71% yield) with TON = 440. Acetophenone was also reduced to 1-phenylethanol using $\text{KOH}/i\text{PrOH}$ under the same conditions with a maximum TON = 472 (Table 2, entry 12). Interestingly, in these runs the decrease in activity associated with Hg(0) poisoning is less important than in the case of CNA reduction (Table 1).

Finally, the hydrogenation protocol already applied to (substituted) acetophenones in our laboratories,¹⁷ namely $t\text{BuOK}/i\text{PrOH}$ under hydrogen pressure (30 bar) at room temperature, was tested for the reduction of acetophenone and 2-cyclohexen-1-one in the presence of **6** (Table 3).

Blank runs (no catalyst, entry 4; no base, entry 5) showed that acetophenone was not reduced without the presence of both a catalyst and a base. $[\text{Ir}(\text{cod})\text{Cl}]_2$ was chosen for control runs and performed poorly (ca. 20% conversion at 4 h) in comparison to **6** (78% conversion, 4 h, TON = 195), which gave almost complete conversion (94%) after 6 h. Reduction of 2-cyclohexen-1-one in the presence of **6** reached 60% conversion, yielding hydrogenation products with a ketone/alcohol ratio of 2.5.

Table 2. Transfer Hydrogenation of BZA, 2-Cyclohexen-1-one, and Acetophenone with 6 using either the HCO₂Na/H₂O/MeOH or the KOH/ⁱPrOH Protocol

entry	substrate	conversn (%) (time (h))	yield (%)			TON (av)
			A ^c	B ^c	C ^c	
1	BZA ^a	25.5 (5)	21.1	4.4	0.0	26
2	BZA ^a	55.1 (24)	43.7	11.5	0.0	55
3	2-cyclohexen-1-one ^a	31.0 (5)	24.6	0.1	0.9	31
4	2-cyclohexen-1-one ^a	67.4 (24)	57.9	0.2	6.3	67
5	2-cyclohexen-1-one ^{a,d}	25.6 (5)	29.7	0.1	1.2	26
6	2-cyclohexen-1-one ^{a,d}	64.4 (24)	60.0	0.2	7.2	64
7	2-cyclohexen-1-one ^b	83.3 (5)	24.9	0.6	57.8	416
8	2-cyclohexen-1-one ^b	88.1 (24)	16.3	0.5	71.3	440
9	2-cyclohexen-1-one ^{b,d}	79.6 (5)	29.5	0.5	49.6	398
10	2-cyclohexen-1-one ^{b,d}	87.8 (24)	22.0	0.5	65.3	439
11	acetophenone ^b	84.5 (5)	84.5			422
12	acetophenone ^b	94.5 (24)	94.5			472
13	acetophenone ^{b,d}	83.8 (5)	83.8			419
14	acetophenone ^{b,d}	94.2 (24)	94.2			471

^a Conditions: substrate, 0.75 mmol; catalyst, 7.5×10^{-3} mmol; HCO₂Na, 7.5 mmol; MeOH/H₂O (1:1), 6 mL. ^b Conditions: substrate, 4.40 mmol; catalyst, 8.8×10^{-3} mmol; KOH, 0.88 mmol; ⁱPrOH, 8.8 mL. ^c GC values based on pure samples. For BZA: A = 4-phenyl-2-butanone; B = 4-phenyl-3-buten-2-ol; C = 4-phenyl-2-butanol, *T* = 60 °C. For 2-cyclohexen-1-one: A = cyclohexanone; B = 2-cyclohexen-1-ol; C = cyclohexanol, *T* = 80 °C. For acetophenone: A = 1-phenylethanol, *T* = 80 °C. ^d One drop of Hg(0) added.

Table 3. Hydrogenation of 2-Cyclohexen-1-one and Acetophenone with 6 in ⁱPrOH/^tBuOK under a Pressure of H₂

entry	substrate	conversn (%) (time (h))	yield (%)			TON (av)
			A ^b	B ^b	C ^b	
1	acetophenone ^a	78.3 (4)	78.3			195
2	acetophenone ^a	94.1 (6)	94.1			240
3	acetophenone ^c	19.6 (4)	19.6			47
4	acetophenone ^d	<1 (4)	<1			0
5	acetophenone ^e	<1 (4)	<1			0
6	acetophenone ^{a,f}	76.2 (4)	76.2			191
7	2-cyclohexen-1-one ^a	60.1 (4)	42.5	0.9	16.7	150
8	2-cyclohexen-1-one ^d	19.8 (4)	17.1	0.0	2.7	50
9	2-cyclohexen-1-one ^e	17.1 (6)	17.1	0.0	0.0	43
10	2-cyclohexen-1-one ^{a,f}	59.5 (4)	36.0	0.4	23.1	149

^a Conditions: substrate, 1.75 mmol; catalyst, 7.0×10^{-3} mmol; ^tBuOK, 0.35 mmol; ⁱPrOH, 2 mL. *p*(H₂), 30 bar; 25 °C. ^b GC values based on pure samples. For 2-cyclohexen-1-one: A = cyclohexanone; B = 2-cyclohexen-1-ol; C = cyclohexanol. For acetophenone: A = 1-phenylethanol. For cinnamaldehyde: A = hydrocinnamaldehyde; B = cinnamol; C = 3-phenyl-1-propanol. ^c As above, catalyst [Ir(cod)Cl]₂. ^d As above, no catalyst. ^e As above, no base. ^f One drop of Hg(0) added.

3. CONCLUSIONS

In summary, examples of coordination to Ir(I) of water-soluble β-phosphino alcohols such as (SR,RS)-PZA-NMe₂ and PZA, members of the class of “upper rim” derivatized analogues of

the well-known phosphine PTA, were obtained. A combination of experimental and theoretical data suggest that in polar solvents κ¹P-[IrCl(cod)(L)] may easily displace the chloride ligand to form the cationic κ²P,O-[Ir(cod)(L)]⁺, which in turn may be in equilibrium with an isomer containing the ligand L in a zwitterionic NH⁺⋯O⁻ form. The precatalysts were tested for the hydrogenation of α,β-unsaturated aldehydes and ketones, including acetophenone, using different mild reduction protocols such as transfer hydrogenation with sodium formate, the classic ⁱPrOH/KOH, and a combined hydrogenation/transfer hydrogenation protocol, run at room temperature under a pressure of 30 bar of H₂ and in the presence of ^tBuOK as base in ⁱPrOH. When aqueous conditions were used, Hg(0) poisoning experiments showed that a mixed homogeneous/heterogeneous system may be active under the conditions applied for the catalytic tests, especially for cinnamaldehyde reduction. Current studies are in progress to obtain more stable water-soluble transition-metal complexes based on different “upper rim” functionalizations of PTA.

4. EXPERIMENTAL SECTION

4.1. General Methods and Materials. All synthetic procedures were carried out using standard Schlenk techniques under an inert atmosphere of dry nitrogen. All glassware was dried overnight in the oven. PTA,⁴ PZA,¹⁶ and [Ir(cod)Cl]₂³⁹ were prepared as described in the literature. All solvents were distilled and degassed prior to use according to standard procedures.⁴⁰ Doubly distilled water was used. Deuterated solvents and other reagents were bought from commercial suppliers and used without further purification. Column chromatographic purification was performed using glass columns (10–50 mm wide) and silica gel (230–400 mesh particle size). The ¹H, ¹³C{¹H}, and ³¹P{¹H} NMR were recorded on a Bruker Avance II 300 spectrometer (operating at 300.13, 75.47, and 121.50 MHz, respectively) and a Bruker Avance II 400 spectrometer (operating at 400.13, 100.61, and 161.98 MHz, respectively). Peak positions are relative to tetramethylsilane and were calibrated against the residual solvent resonance (¹H) or the deuterated solvent multiplet (¹³C). ³¹P{¹H} NMR was referenced to 85% H₃PO₄, with the downfield shift taken as positive. All of the NMR spectra were recorded at room temperature (20 °C). IR spectra (KBr pellets) were recorded on a Perkin-Elmer Spectrum BX II series FT-IR spectrophotometer in the range 4000–400 cm⁻¹. Elemental analyses were performed on a Perkin-Elmer 2400 series II elemental analyzer. ESI-MS spectra were measured on a LCQ Orbitrap mass spectrometer (ThermoFischer, San Jose, CA) equipped with a conventional ESI source by direct injection of the sample solution and are reported in the form *m/z* (intensity relative to base 100). Conductivities were measured with an Orion Model 990101 conductance cell connected to a Model 101 conductivity meter. GC analyses were performed on a Shimadzu 2010 gas chromatograph (with polar column) equipped with a flame ionization detector and a VF-WAXms capillary column (30 m, 0.25 mm i.d., 0.25 μm film thickness), on a Shimadzu GC-14A gas chromatograph (with apolar column) equipped with a flame ionization detector and an SPB-1 Supelco fused silica capillary column (30 m, 0.25 mm i.d., 0.25 μm film thickness), and on a Shimadzu GC-17A gas chromatograph (with a chiral column Lipodex-E Macherey-Nagel) equipped with a flame ionization detector (50 m, 0.25 mm i.d., 0.40 mm o.d.).

4.2. Improved Synthesis of (1,3,5-Triaza-7-phosphaadamantane-6-yl)lithium (1; PTA-Li). The synthetic protocol described in the literature¹⁴ has been modified. PTA (1.57 g, 10.0 mmol) was completely dissolved in dry and degassed benzene (160 mL) at 50 °C with strong stirring. The solution was then cooled to approximately 30 °C, and *n*-butyllithium solution (1.6 M solution in hexanes, 10 mL, 16 mmol) was slowly added. After a few minutes a white solid was formed and the reaction mixture was stirred at room temperature for 2 h. The

solid was filtered on a frit under nitrogen and washed with dry *n*-pentane (3 × 30 mL). PTA-Li was obtained in quantitative yield (1.63 g). Due to its highly pyrophoric nature and reactivity with atmospheric moisture, the solid must be stored under nitrogen and the batch consumed within a few days. **CAUTION!** The compound ignites spontaneously if exposed to air and is very sensitive to moisture. A protective nitrogen atmosphere and gloves must be used at all times for storage and handling.

4.3. Synthesis of (4'-(Dimethylamino)phenyl)(1,3,5-triaza-7-phosphatricyclo[3.3.1.1]dec-6-yl)methanol (2; PZA-NMe₂). In a 100 mL Schlenk flask, **1** (1.80 g, 11.0 mmol) was suspended in 30 mL of dry THF and maintained in a liquid nitrogen/acetone bath at -78 °C under an inert atmosphere of nitrogen. 4-(Dimethylamino)benzaldehyde (1.80 g, 12.1 mmol) was dissolved in 10 mL of dry THF, cooled to 0 °C, and transferred via cannula to the slurry. The resulting yellow mixture was left at -78 °C for 15 min and then warmed to reach room temperature and stirred for an additional 2 h. A 0.5 mL portion of doubly distilled water was added to quench the reaction, and the solvent was removed under reduced pressure. The resulting solid was washed with acetone (10 mL) to give a pale yellow powder (2.10 g, 62% yield) containing the two diastereoisomers. Silica gel flash column chromatography gave pure product **2** (1.40 g, 41% yield) (*R_f* = 0.23, eluent MeOH). The major diastereoisomer **2a** was obtained pure after fractional crystallization from CH₂Cl₂ (0.77 g, white powder, 23% yield) and fully characterized. Crystals suitable for X-ray diffraction were obtained by the slow evaporation under nitrogen of a solution of **2a** in CH₂Cl₂ and EtOH. *S*(H₂O)_{20 °C} = 1.9 g/L. Data for the major diastereoisomer (*SR,RS*)-**2a** are as follows. ¹H NMR (CDCl₃, 400.13 MHz): δ 7.35 (d, ³J_{HH} = 8.6 Hz, 2H, Ar); 6.74 (d, ³J_{HH} = 8.6 Hz, 2H, Ar); 5.16 (dd, ³J_{HH} = 3.7 Hz, ³J_{HP} = 8.4 Hz, 1H, CHOH); 4.85 (AB system, ²J_{H_AH_B} = 13.4 Hz, 2H, NCH₂N); 4.57–4.37 (m, 4H, NCH₂N); 4.29–4.24 (m, 1H, PCH₂N); 4.15–4.08 (m, 1H, PCH₂N); 3.90–3.80 (m, 3H, PCH₂N + PCHN); 2.97 (s, 6H, N(CH₃)₂). ³¹P{¹H} NMR (CDCl₃, 161.98 MHz): δ -102.72 (s). ³¹P{¹H} NMR (D₂O, 121.50 MHz): δ -99.07 (s). ¹³C{¹H} NMR (100.61 MHz, CDCl₃): δ 150.42 (s, Ar); 130.51 (s, Ar); 127.24 (s, Ar); 112.30 (s, Ar); 77.64 (d, ²J_{CP} = 6.5 Hz, CHOH); 74.20 (s, NCH₂N); 67.78 (s, NCH₂N); 65.75 (d, ¹J_{CP} = 23.1 Hz, PCHN); 51.55 (d, ¹J_{CP} = 19.9 Hz, PCH₂N); 48.43 (d, ¹J_{CP} = 24.0 Hz, PCH₂N); 40.54 (s, N(CH₃)₂). Anal. Found (calcd for C₁₅H₂₃N₄OP) (306.34 g mol⁻¹): C, 58.67 (58.81); H, 7.55 (7.57); N, 18.58 (18.29). ESI-MS (*m/z* (%)): 307.06 (7) [M⁺], 246.02 (100) [C₁₃H₁₇N₃P⁺]. IR (KBr, cm⁻¹): ν_{OH} 3401 (br, s); ν_{arom} 1612 (s), 1525 (s).

4.4. Synthesis of (SR,RS)-(4'-(Dimethylamino)phenyl)-(1,3,5-triaza-7-phosphatricyclo[3.3.1.1]dec-6-yl)methanol Oxide (3; O=PZA-NMe₂). In a one-necked round-bottomed flask containing ligand **2a** (0.55 g, 1.8 mmol), methanol (140 mL) was added and the mixture was slightly heated to dissolve the solid. The solution was cooled to room temperature, and an excess of aqueous H₂O₂ (35%, 260 μL) diluted in ethanol (8 mL) was slowly added. The reaction mixture was stirred at room temperature for 1 h, and a small amount of a white precipitate appeared. The solvent was then removed by rotary evaporation, yielding 0.52 g (90%) of pure product. *S*(H₂O)_{20 °C} = 12.5 g/L. ¹H NMR (400.13 MHz, D₂O): δ 7.33 (d, ³J_{HH} = 8.2 Hz, 2H, Ar); 6.94 (d, ³J_{HH} = 8.2 Hz, 2H, Ar); 5.34 (dd, ³J_{HP} = 10.9 Hz, ³J_{HH} = 3.4 Hz, 1H, CHOH); 4.19 (AB system, ²J_{H_AH_B} = 14.0 Hz, 2H, NCH₂N); 4.31–4.10 (m, 6H, NCH₂N + PCH₂N); 3.89–3.77 (m, 3H, PCH₂N + PCHN); 2.79 (s, 6H, N(CH₃)₂). ³¹P{¹H} NMR (161.98 MHz, D₂O): δ 2.09 (s). ¹³C{¹H} NMR (100.61 MHz, D₂O): δ 151.44 (s, Ar); 131.44 (d, ³J_{CP} = 7.1 Hz, Ar); 127.57 (s, Ar); 115.52 (s, Ar); 72.97 (d, ²J_{CP} = 2.3 Hz, CHOH); 72.44 (d, ³J_{CP} = 6.1 Hz, NCH₂N); 70.45 (d, ³J_{CP} = 8.4 Hz, NCH₂N); 68.50 (d, ¹J_{CP} = 50.7 Hz, PCHN); 64.89 (d, ³J_{CP} = 11.6 Hz, NCH₂N); 53.31 (d, ¹J_{CP} = 52.7 Hz, PCH₂N); 50.79 (d, ¹J_{CP} = 52.0 Hz, PCH₂N); 40.96 (s, N(CH₃)₂). Anal. Found (calcd for C₁₅H₂₃N₄O₂P) (322.34 g mol⁻¹): C, 56.24 (55.89); H, 7.88 (7.19); N, 17.67 (17.38). IR (KBr, cm⁻¹): ν_{OH} 3227 (br, m); ν_{arom} 1613 (s), 1525 (s); ν_{P=O} 1155 (m).

4.5. Synthesis of (SR,RS)-(4'-(Dimethylamino)phenyl)-(1,3,5-triaza-7-phosphatricyclo[3.3.1.1]dec-6-yl)methanol Sulfide (4; S=PZA-NMe₂).

In a three-necked round bottomed flask equipped with a reflux condenser, **2a** (0.50 g, 1.6 mmol) was dissolved in degassed water (150 mL) and heated to 90 °C to completely dissolve the compound. An excess of elemental sulfur (0.13 g, 4.1 mmol of S) was added and the suspension refluxed for 90 min with strong stirring. The reaction mixture was cooled to room temperature and the precipitate filtered on a Büchner funnel. The solid was washed with hot CCl₄ (2 × 3 mL) and dried under vacuum, yielding a white solid (0.35 g, 65%). *S*(H₂O)_{20 °C} = 0.5 g/L. ¹H NMR (400.13 MHz, DMSO-*d*₆): δ 7.30 (d, ³J_{HH} = 8.5 Hz, 2H, arom); 6.66 (d, ³J_{HH} = 8.5 Hz, 2H, arom); 5.32 (dd, ³J_{HP} = 10.1 Hz, ³J_{HH} = 3.6 Hz, 1H, CHOH); 4.39–4.18 (m, 7H, NCH₂N + PCH₂N); 4.00–3.84 (m, 4H, PCH₂N + PCHN); 2.87 (s, 6H, N(CH₃)₂). ³¹P{¹H} NMR (161.98 MHz, DMSO-*d*₆): δ -14.07 (s). ¹³C{¹H} NMR (100.61 MHz, DMSO-*d*₆): δ 150.26 (s, Ar); 130.43 (d, ³J_{CP} = 6.8 Hz, Ar); 128.48 (s, Ar); 112.27 (s, Ar); 74.85 (s, CHOH); 73.82 (d, ³J_{CP} = 5.8 Hz, NCH₂N); 71.71 (d, ³J_{CP} = 9.2 Hz, NCH₂N); 70.17 (d, ¹J_{CP} = 31.4 Hz, PCHN); 65.92 (d, ³J_{CP} = 12.6 Hz, NCH₂N); 58.11 (d, ¹J_{CP} = 35.4 Hz, PCH₂N); 55.36 (d, ¹J_{CP} = 34.5 Hz, PCH₂N); 40.73 (s, N(CH₃)₂). Anal. Found (calcd for C₁₅H₂₃N₄OPS) (338.41 g mol⁻¹): C, 53.71 (53.24); H, 6.93 (6.85); N, 16.71 (16.56). IR (KBr, cm⁻¹): ν_{OH} 3360 (vs); ν_{arom} 1615 (s), 1529 (s); ν_{P=S} 646 (m).

4.6. Synthesis of [Ir(cod)Cl(PZA)] (5). In a Schlenk tube under nitrogen, a solution of [Ir(cod)Cl]₂ (0.26 g, 0.4 mmol) in toluene (5 mL) was added by cannula to a solution of PZA (0.20 g, 0.8 mmol) in CH₂Cl₂ (10 mL). The solution was stirred at room temperature for 1 h, after which the volume was reduced to approximately a third, resulting in the formation of an orange precipitate. The suspension was filtered and the product washed once with ice-cold toluene and then twice with *n*-pentane and dried under vacuum (0.33 g, 74% yield). *S*(H₂O)_{20 °C} = 3.4 g/L. Spectroscopic data for compound **5** (two diastereoisomers, 1:2 ratio, values for minor isomer in parentheses) are as follows. ¹H NMR (400.13 MHz, CD₂Cl₂): δ 7.13–7.42 (m, 5H, Ar); 5.32–5.26 (s, 6.68–5.63) (m, 2H, NCH₂N); 5.18–5.09 (m, 2H, cod + CHOH); 5.08–4.84 (m, 3H, cod); 4.62–4.43 (m, 2H, NCH₂N); 4.38–4.19 (m, 3H, NCH₂N + PCHN); 4.12–3.84 (m, 4H, PCH₂N); 2.32–2.08 (m, 4H, cod); 1.94–1.64 (m, 4H, cod). ³¹P{¹H} NMR (161.98 MHz, CD₂Cl₂): δ -64.97 (-58.50) (s). ¹³C{¹H} NMR (100.61 MHz, CD₂Cl₂): δ 140.88 (140.97) (s, Ar); 128.26 (128.02) (s, Ar); 127.89 (127.36) (s, Ar); 127.15 (126.91) (s, Ar); 97.93 (d, ²J_{CP} = 16.9 Hz, cod); 97.20 (d, ²J_{CP} = 17.5 Hz, cod); 75.65 (s, NCH₂N); 73.83 (d, ³J_{CP} = 7.7 Hz, NCH₂N); 72.83 (s, NCH₂N); 67.65 (d, ¹J_{CP} = 41.9 Hz, PCHN); 67.48 (d, ²J_{CP} = 28.8 Hz, CHOH); 49.59 (49.98) (d, ¹J_{CP} = 24.4 Hz, PCH₂N); 44.82 (46.0) (d, ¹J_{CP} = 23.0 Hz, PCH₂N); 34.60 (34.26) (s, cod); 33.11 (33.66) (s, cod); 29.58 (28.95) (s, cod); 28.59 (27.98) (s, cod). Anal. Found (calcd for C₂₁H₃₀ClIrN₃OP) (599.13 g mol⁻¹): C, 41.86 (42.10); H, 4.94 (5.05); N, 7.06 (7.01). MS (nESI⁺; *m/z*): 564.2 [Ir(cod)(PZA)]⁺. IR (KBr, cm⁻¹): ν_{OH} 3433 (br, s); ν_{arom} 1610 (s), 1524 (s).

4.7. Synthesis of [Ir(cod)Cl{(SR,RS)-(PZA-NMe₂)}] (6). A Schlenk tube was charged under nitrogen with ligand **2a** (0.20 g, 0.6 mmol) and [Ir(cod)Cl]₂ (0.22 g, 0.3 mmol). Dry degassed CH₂Cl₂ (15 mL) was added, and the resulting yellow solution was stirred at room temperature for 1 h 30 min. The solution was concentrated under vacuum to half of the volume, and dry *n*-pentane (10 mL) was added. The yellow precipitate was filtered on a frit, washed with cold *n*-pentane, and dried under vacuum, yielding 0.26 g of the complex (67% yield). *S*(H₂O)_{20 °C} = 1.7 g/L. ¹H NMR (300.13 MHz, CDCl₃): δ 7.33 (d, ³J_{HH} = 8.6 Hz, 2H, Ar); 6.72 (d, ³J_{HH} = 8.6 Hz, 2H, Ar); 5.30–5.16 (br m, 2H, NCH₂N + cod); 5.04–5.01 (m, 1H, cod); 4.67–4.44 (m, 6H, NCH₂N + PCHN + CHOH); 4.35–3.87 (m, 7H, cod + PCH₂N); 2.95 (s, 6H, N(CH₃)₂); 2.25–1.68 (m, 8H, CH₂, cod). ³¹P{¹H} NMR (121.50 MHz, CDCl₃): δ -64.09 (s). ³¹P{¹H} NMR (121.50 MHz, D₂O): δ -18.12 (s). ¹³C{¹H} NMR (75.47 MHz, CDCl₃): δ 150.36 (s, Ar);

127.91 (s, Ar); 127.56 (d, $^3J_{\text{CP}} = 6.9$ Hz, Ar); 112.26 (s, Ar); 98.07 (d, $^2J_{\text{CP}} = 12.8$ Hz, cod); 97.13 (d, $^2J_{\text{CP}} = 13.7$ Hz, cod); 75.74 (d, $^3J_{\text{CP}} = 4.2$ Hz, NCH₂N); 73.98 (d, $^3J_{\text{CP}} = 6.0$ Hz, NCH₂N); 72.97 (d, $^3J_{\text{CP}} = 3.9$ Hz, NCH₂N); 67.52 (d, $^1J_{\text{CP}} = 17.3$ Hz, PCHN); 67.32 (d, $^2J_{\text{CP}} = 8.3$ Hz, CHOH); 49.76 (d, $^1J_{\text{CP}} = 18.2$ Hz, PCH₂N); 44.89 (d, $^1J_{\text{CP}} = 17.3$ Hz, PCH₂N); 40.49 (s, N(CH₃)₂); 34.62 (d, $^3J_{\text{CP}} = 3.6$ Hz, cod); 33.09 (d, $^3J_{\text{CP}} = 3.0$ Hz, cod); 29.65 (d, $^3J_{\text{CP}} = 2.1$ Hz, cod); 27.98 (d, $^3J_{\text{CP}} = 4.2$ Hz, cod). Anal. Found (calcd for C₂₃H₃₅ClIrN₄OP) (642.19 g mol⁻¹): C, 43.48 (43.02); H, 5.67 (5.49); N, 8.58 (8.72). MS (nESI⁺; *m/z*): 605.3 [Ir(cod)(PZA-NMe₂)⁺]. IR (KBr, cm⁻¹): ν_{OH} 3423 (br, s); ν_{arom} 1613 (m), 1524 (m).

4.8. X-ray Diffraction Data for (SR,RS)-PZA-NMe₂ (2a). X-ray data collection for compound **2a** was carried out at room temperature by using a CCD diffractometer equipped with Mo K α radiation (0.710 73 Å). The program CrysAlis CCD⁴¹ and CrysAlis RED⁴² were used for data collection and reduction, respectively. Absorption correction was applied through the program ABSPACK.⁴² The structure solution was obtained by using the direct methods in Sir97.⁴³ Structure refinement was performed with SHELXL⁴⁴ by using the full-matrix least-squares method for all the available *F*² data. All of the non-hydrogen atoms were refined anisotropically, and the H atoms bonded to the carbon atoms were fixed in calculated positions and refined isotropically with thermal factors 20% larger (50% for the H of the methyl groups) than those of the atoms to which they are bound. The hydrogen atom of the OH was located in the Fourier difference map, and its coordinate was freely refined. All calculations were performed with the WINGX package.⁴⁵ The molecular drawings were made by using both ORTEP-III for Windows⁴⁶ and SCHAKAL97.⁴⁷

4.9. Transfer Hydrogenation Tests. The reactions were carried out in Schlenk tubes under an inert atmosphere using degassed solvents. For transfer hydrogenation of cinnamaldehyde (CNA) and 2-cyclohexen-1-one, the catalyst and HCO₂Na were placed in two different Schlenk tubes, to which 3 mL of a H₂O/MeOH mixture was added (1/1 or 1/2 as specified in Table 1) after three freeze–thaw–pump cycles. The formate solution was added by cannula to the solution of catalyst, and the temperature was set. The liquid substrate was directly added by syringe to the reaction mixture. In the case of benzylideneacetone (BZA), HCO₂Na was dissolved in 2 mL of water and added via cannula to the solution of catalyst in MeOH (2 mL). The temperature was set, and the solution of BZA in MeOH (2 mL) was added to the mixture. At the end of the catalytic runs, an aliquot of the reaction mixture (0.1 mL) was taken by syringe and diluted with methanol (0.4 mL) or extracted with dichloromethane and analyzed by GC. For the hydrogenation of 2-cyclohexen-1-one and acetophenone with KOH/¹PrOH, the catalyst and the base were placed in a Schlenk tube and dissolved in dry isopropyl alcohol (ca. 9 mL). When the reaction temperature was reached, the substrate was slowly added by syringe. At the end of the reaction, an aliquot of the mixture was taken, diluted with MeOH, and analyzed by GC. The aliquots were usually passed through a plug of silica before the injection to remove traces of metal. Each test was repeated twice to check for reproducibility.

4.10. Autoclave Hydrogenation Experiments. A multisample batch setup was used for these experiments. Solid catalysts and ^tBuOK were placed under nitrogen in separate glass vials (7 × 3 mL), each equipped with a stirring bar, co-located in a Teflon carousel placed in a home-built stainless steel autoclave (100 mL). Dry isopropyl alcohol (2 mL) and the substrate were added by syringe, and the autoclave was sealed. After three cycles of purging with hydrogen, the autoclave was pressurized to 30 bar of H₂. The catalytic tests were started by leaving the autoclave with stirring at room temperature for the chosen time. The pressure was then released, and an aliquot of the reaction mixture (0.1 mL) was taken from each vial, diluted with methanol (0.4 mL), and analyzed by GC. Each test was repeated twice to check for reproducibility.

■ ASSOCIATED CONTENT

S Supporting Information. Tables, figures, and a CIF file giving Cartesian coordinates for all the considered complexes **6a–f** and crystal data and structure refinement details for **2a**. This material is available free of charge via the Internet at <http://pubs.acs.org>.

■ AUTHOR INFORMATION

Corresponding Author

*E-mail: lgonsalvi@iccom.cnr.it (L.G.); mperuzzini@iccom.cnr.it (M.P.).

■ ACKNOWLEDGMENT

We thank the Italian Ministries MIUR and MATTM and the Ente Cassa di Risparmio di Firenze (ECRF) for financial support through the PRIN 2007, PIRODE, and FIRENZE HYDROLAB projects, respectively. Thanks are expressed to the EC for promoting this scientific activity through the FP6 Research Training Network AQUACHEM (contract MCRTN-2003-503864). The GDRE project “Catalyse Homogène pour le Développement Durable (CH2D)” and COST Action CM0802 “PhoSciNet” are also thanked for funding mobility. L.G. thanks the MAE for a JRP grant within the Executive Programme of Cooperation Italy-USA (2008–2010). M.E. thanks the foundation Bengt Lundqvist minne (Sweden) for extra financial support. D.A.K. thanks the donors of the Petroleum Research Fund, administered by the American Chemical Society, and Fulbright Research Scholarships (2009–2010) for partial support of this research. A.I. thanks the ISCRA-CINECA HP grant “HP10BNL89W” for computational time.

■ REFERENCES

- (1) Anastas, P. T.; Kirchoff, M. M. *Acc. Chem. Res.* **2002**, *35*, 686–694.
- (2) (a) Joó, F. *Acc. Chem. Res.* **2002**, *35*, 738–745. (b) Joó, F. *Aqueous Organometallic Catalysis*; Kluwer: Dordrecht, The Netherlands, 2001. (c) Cornils, B.; Hermann, W. A., Eds. *Aqueous-Phase Organometallic Catalysis*, 2nd ed.; Wiley-VCH: Weinheim, Germany, 2004. (d) Horvath, I. T.; Joó, F., Eds. *Aqueous Organometallic Chemistry and Catalysis*; Kluwer: Dordrecht, The Netherlands, 1995; NATO ASI 3/5.
- (3) For a recent comprehensive review on water-soluble ligands and applications in catalysis see: Shaughnessy, K. H. *Chem. Rev.* **2009**, *109*, 643–710.
- (4) (a) Daigle, D. J.; Pepperman, A. B., Jr.; Vail, S. L. *J. Heterocycl. Chem.* **1974**, *11*, 407–408. (b) Daigle, D. J. *Inorg. Synth.* **1998**, *32*, 40–42.
- (5) (a) Phillips, A. D.; Gonsalvi, L.; Romerosa, A.; Vizza, F.; Peruzzini, M. *Coord. Chem. Rev.* **2004**, *248*, 955–993. (b) Bravo, J.; Bolaño, S.; Gonsalvi, L.; Peruzzini, M. *Coord. Chem. Rev.* **2010**, *254*, 555–607.
- (6) (a) Bolaño, S.; Gonsalvi, L.; Zanobini, F.; Vizza, F.; Bertolasi, V.; Romerosa, A.; Peruzzini, M. *J. Mol. Catal. A: Chem.* **2004**, *224*, 61–70. (b) Horváth, H.; Laurenzy, G.; Katho, A. *J. Organomet. Chem.* **2004**, *689*, 1036–1045. (c) Mebi, C. A.; Frost, B. J. *Organometallics* **2005**, *24*, 2339–2346. (d) Krogstad, D. A.; Cho, J.; DeBoer, A. J.; Klitzke, J. A.; Sanow, W. R.; Williams, H. A.; Halfen, J. A. *Inorg. Chim. Acta* **2006**, *359*, 136–148. (e) Krogstad, D. A.; Owens, S. B.; Halfen, J. A.; Young, V. G., Jr. *Inorg. Chem. Commun.* **2005**, *8*, 65–69. (f) Krogstad, D. A.; DeBoer, A. J.; Ortmeier, W. J.; Rudolf, J. W.; Halfen, J. A. *Inorg. Chem. Commun.* **2005**, *8*, 1141–1144. (g) Ruiz, J.; Cutillas, N.; López, F.; López, G.; Bautista, D. *Organometallics* **2006**, *25*, 5768–5773. (h) Korthals, B.; Göttker-Schnetmann, I.; Mecking, S. *Organometallics* **2007**, *26*, 1311–1316. (i) Mebi, C. A.; Nair, R. P.; Frost, B. J. *Organometallics* **2007**, *26*, 429–438.

- (7) (a) Ang, W. H.; Daldini, E.; Sclaro, C.; Scopelliti, R.; Juillerat-Jennerat, L.; Dyson, P. J. *Inorg. Chem.* **2006**, *45*, 9006–9013. (b) Sclaro, C.; Bergamo, A.; Brescacin, L.; Delfino, R.; Cocchietto, M.; Laurenczy, G.; Geldbach, T. J.; Sava, G.; Dyson, P. J. *J. Med. Chem.* **2005**, *48*, 4161–4171. (c) Dorcier, A.; Dyson, P. J.; Gossens, C.; Rothlisberger, U.; Scopelliti, R.; Tavernelli, I. *Organometallics* **2005**, *24*, 2114–2123. (d) Dorcier, A.; Ang, W. H.; Bolaño, S.; Gonsalvi, L.; Juillerat-Jennerat, L.; Laurenczy, G.; Peruzzini, M.; Phillips, A. D.; Zanobini, F.; Dyson, P. J. *Organometallics* **2006**, *25*, 4090–4096. (e) Ang, W. H.; Dyson, P. J. *Eur. J. Inorg. Chem.* **2006**, 4003–4018. (f) Romerosa, A.; Campos-Malpartida, T.; Lidrissi, C.; Saoud, M.; Serrano-Ruiz, M.; Peruzzini, M.; Garrido-Cardenas, J. A.; García-Maroto, F. *Inorg. Chem.* **2006**, *45*, 1289–1298. (g) Romerosa, A.; Saoud, M.; Campos-Malpartida, T.; Lidrissi, C.; Serrano-Ruiz, M.; Peruzzini, M.; Garrido, J. A.; García-Maroto, F. *Eur. J. Inorg. Chem.* **2007**, 2803–2812. (h) Casini, A.; Edefe, F.; Erlandsson, M.; Gonsalvi, L.; Marrone, A.; Ciancetta, A.; Re, N.; Ienco, A.; Messori, L.; Peruzzini, M.; Dyson, P. J. *Dalton Trans.* **2010**, *39*, 5556–5563.
- (8) Gutkin, V.; Gun, J.; Prikhodchenko, P. V.; Lev, O.; Romerosa, A.; Campos Malpartida, T.; Lidrissi, C.; Gonsalvi, L.; Peruzzini, M. *J. Electrochem. Soc.* **2007**, *154*, F7–F15.
- (9) (a) Rossin, A.; Gonsalvi, L.; Phillips, A. D.; Maresca, O.; Lledos, A.; Peruzzini, M. *Organometallics* **2007**, *26*, 3289–3296. (b) Kovacs, G.; Rossin, A.; Gonsalvi, L.; Lledos, A.; Peruzzini, M. *Organometallics* **2010**, *29*, 5121–5131.
- (10) (a) Daigle, D. J.; Pepperman, A. B., Jr. *J. Heterocycl. Chem.* **1975**, *12*, 579–580. (b) Fluck, E.; Weissgräber, H. J. *Chem. Ztg.* **1977**, *101*, 304. (c) Fluck, E.; Förster, J. E.; Weidlein, J.; Hädicke, E. Z. *Naturforsch.* **1977**, *32*, 499–506. (d) Forward, J. M.; Staples, R. J.; Fackler, J. P., Jr. *Z. Kristallogr.* **1996**, *211*, 129–130. (e) Smolenski, P.; Pruchnik, F. P.; Ciunik, Z.; Lis, T. *Inorg. Chem.* **2003**, *42*, 3318–3322.
- (11) (a) Daigle, D. J.; Boudreaux, G. J.; Vail, S. L. *J. Chem. Eng. Data* **1976**, *21*, 240–241. (b) Siele, V. I. *J. Heterocycl. Chem.* **1977**, *14*, 337–339. (c) Navech, J.; Krammer, R.; Majoral, J. P. *Tetrahedron Lett.* **1980**, *21*, 1449–1452. (d) Darensbourg, D. J.; Yarbrough, J. C.; Lewis, S. J. *Organometallics* **2003**, *22*, 2050–2056.
- (12) (a) Assmann, B.; Angermaier, K.; Schmidbaur, H. *J. Chem. Soc., Chem. Commun.* **1994**, 941–942. (b) Assmann, B.; Angermaier, K.; Paul, M.; Schmidbaur, H. *Chem. Ber.* **1995**, *128*, 891–900. (c) Phillips, A. D.; Bolaño, S.; Bosquain, S. S.; Daran, J.-C.; Malacea, R.; Peruzzini, M.; Poli, R.; Gonsalvi, L. *Organometallics* **2006**, *25*, 2189–2200. (d) Caporali, M.; Bianchini, C.; Bolaño, S.; Bosquain, S. S.; Gonsalvi, L.; Oberhauser, W.; Rossin, A.; Peruzzini, M. *Inorg. Chim. Acta* **2008**, *361*, 3017–3023.
- (13) Mena-Cruz, A.; Lorenzo-Luis, P.; Romerosa, A.; Saoud, M.; Serrano-Ruiz, M. *Inorg. Chem.* **2007**, *46*, 6120–6128.
- (14) Wong, G. W.; Harkreader, J. L.; Mebi, C. A.; Frost, B. J. *Inorg. Chem.* **2006**, *45*, 6748–6755.
- (15) Wong, G. W.; Lee, W.-C.; Frost, B. J. *Inorg. Chem.* **2008**, *47*, 612–620.
- (16) Erlandsson, M.; Gonsalvi, L.; Ienco, A.; Peruzzini, M. *Inorg. Chem.* **2008**, *47*, 8–10.
- (17) Le Roux, E.; Malacea, R.; Manoury, E.; Poli, R.; Gonsalvi, L.; Peruzzini, M. *Adv. Synth. Catal.* **2007**, *349*, 309–313.
- (18) Darensbourg, D. J.; Beckford, F. A.; Reibenspies, J. H. *J. Cluster Sci.* **2000**, *11*, 95–107.
- (19) (a) Krogstad, D. A.; Halfen, J. A.; Terry, T. J.; Young, V. G., Jr. *Inorg. Chem.* **2001**, *40*, 463–471. (b) Kovacs, J.; Todd, T. D.; Reibenspies, J. H.; Joó, F.; Darensbourg, D. J. *Organometallics* **2000**, *19*, 3963–3969.
- (20) Leung, D. H.; Bergman, R. G.; Raymond, K. N. *J. Am. Chem. Soc.* **2006**, *128*, 9781–9797.
- (21) Erlandsson, M.; Landaeta, V. R.; Gonsalvi, L.; Peruzzini, M.; Phillips, A. D.; Dyson, P. J.; Laurenczy, G. *Eur. J. Inorg. Chem.* **2008**, 620–627.
- (22) (a) Malacea, R.; Manoury, E.; Poli, R. *Coord. Chem. Rev.* **2010**, *254*, 729–752. (b) Bianchini, C.; Gonsalvi, L.; Peruzzini, M. In *Iridium Complexes in Organic Synthesis*; Oro, L., Claver, C., Eds.; Wiley-VCH: Weinheim, Germany, 2008; pp 55–106.
- (23) Garrou, P. E. *Chem. Rev.* **1981**, *81*, 229–266.
- (24) Isolation of a pure product from the reaction mixture has been troublesome so far, as upon solvent removal and subsequent $^{31}\text{P}\{^1\text{H}\}$ NMR analysis, signals due to unidentified species appear. Work is in progress to purify the solid and obtain suitable crystals for XRD analysis.
- (25) For recent comprehensive volumes on hydrogenation reactions see: (a) Blaser, H. U., Schmidt, E., Eds. *Asymmetric Catalysis on Industrial Scale: Challenges, Approaches and Solutions*; Wiley-VCH: Weinheim, Germany, 2004. (b) de Vries, J. G., Elsevier, C. J., Eds. *Handbook of Homogeneous Hydrogenation*; Wiley-VCH: Weinheim, Germany, 2007.
- (26) For a recent review on asymmetric transfer hydrogenation (ATH) in water see: Wu, X.; Wang, C.; Xiao, J. *Platinum Met. Rev.* **2010**, *54*, 3–19.
- (27) Himeda, Y.; Onozawa-Kumatsuzaki, N.; Miyazawa, S.; Sugihara, H.; Hirose, T.; Kasuga, K. *Chem. Eur. J.* **2008**, *14*, 11076–11081 and references therein.
- (28) (a) Wu, X.; Li, X.; Zanotti-Gerosa, A.; Pettman, A.; Liu, J.; Mills, A. J.; Xiao, J. *Chem. Eur. J.* **2008**, *14*, 2209–2222. (b) Wu, X.; Corcoran, C.; Yang, S.; Xiao, J. *ChemSusChem* **2008**, *1*, 71–74. (c) Ikariya, T.; Murata, K.; Noyori, R. *Org. Biomol. Chem.* **2006**, *4*, 393–406. (d) Fujii, A.; Hashiguchi, S.; Uematsu, N.; Ikariya, T.; Noyori, R. *J. Am. Chem. Soc.* **1996**, *118*, 2521–2522.
- (29) Wu, X.; Li, X.; McConville, M.; Saidi, O.; Xiao, J. *J. Mol. Catal. A: Chem.* **2006**, *247*, 153–158.
- (30) Marchetti, M.; Minello, F.; Paganelli, S.; Piccolo, O. *Appl. Catal. A: Gen.* **2010**, *373*, 76–80.
- (31) Darensbourg, D. J.; Joó, F.; Kannisto, M.; Kathó, A.; Reibenspies, J. H. *Organometallics* **1992**, *11*, 1990.
- (32) Smolenski, P.; Pruchnik, F. P.; Ciunik, Z.; Lis, T. *Inorg. Chem.* **2003**, *42*, 3318–3322.
- (33) Akbayeva, D. N.; Gonsalvi, L.; Oberhauser, W.; Peruzzini, M.; Vizza, F.; Brüggeller, P.; Romerosa, A.; Sava, G.; Bergamo, A. *Chem. Commun.* **2003**, 264–265.
- (34) Mebi, C. A.; Nair, R. P.; Frost, B. J. *Organometallics* **2007**, *26*, 429–438.
- (35) (a) Noyori, R.; Hashiguchi, S. *Acc. Chem. Res.* **1997**, *30*, 97–102. (b) Yamakawa, M.; Ito, H.; Noyori, R. *J. Am. Chem. Soc.* **2000**, *122*, 1466–1478. (c) Noyori, R.; Ohkuma, T. *Angew. Chem., Int. Ed.* **2001**, *40*, 40–73. (d) Noyori, R. *Angew. Chem., Int. Ed.* **2002**, *41*, 2008–2022. (e) Sandoval, C. A.; Ohkuma, T.; Muniz, K.; Noyori, R. *J. Am. Chem. Soc.* **2003**, *125*, 13490–13503. (f) Ikariya, T.; Murata, K.; Noyori, R. *Org. Biomol. Chem.* **2006**, *4*, 393–406. (g) Sandoval, C. A.; Bie, F.; Matsuoka, A.; Yamaguchi, Y.; Hiroshi, N.; Li, Y.; Koichi, K.; Utsumi, N.; Tsutsumi, K.; Ohkuma, T.; Murata, K.; Noyori, R. *Chem. Asian J.* **2010**, *5*, 806–816.
- (36) During the first synthesis of complex **5**, a black precipitate, likely Ir metal, soon formed after mixing the metal precursor with PZA that had not been previously purified by column chromatography. This behavior was not observed for PZA-NMe₂. After purification, the final yield of PZA decreased from the original 59% to 7–10%. On the basis of the final yields, and in view of further work aimed at the chiral resolution of **2a**, complex **6** was synthesized and used in catalytic tests to a greater extent.
- (37) Examples of metal nanoparticles stabilized by PTA have been recently described; see: Debouttière, P.-J.; Martinez, V.; Philippot, K.; Chaudret, B. *Dalton Trans.* **2009**, 10172–10174.
- (38) (a) Whitesides, G. M.; Hackett, M.; Brainard, R. L.; Lavalleye, J.-P. P. M.; Sowinski, A. F.; Izumi, A. N.; Moore, S. S.; Brown, D. W.; Staudt, E. M. *Organometallics* **1985**, *4*, 1819–1830. (b) Hamlin, J. E.; Hirai, K.; Gibson, V. C.; Maitlis, P. M. *J. Mol. Catal.* **1982**, *15*, 337–347. (c) Lin, Y.; Finke, R. G. *Inorg. Chem.* **1994**, *33*, 4891–4910.
- (39) Herde, J. L.; Lambert, J. C.; Senoff, C. V. *Inorg. Synth.* **1974**, *15*, 18–19.
- (40) Perrin, D. D.; Armarego, W. L. F. *Purification of Laboratory Chemicals*, 3rd ed.; Pergamon: New York, 1988.
- (41) *CrysAlisCCD, Version 1.171.31.2 (release 07-07-2006 CrysAlis171.NET)*; Oxford Diffraction Ltd.
- (42) *CrysAlis RED, Version 1.171.31.2 (release 07-07-2006 CrysAlis171.NET)*; Oxford Diffraction Ltd.

(43) Altomare, A.; Burla, M. C.; Camalli, M.; Cascarano, G. L.; Giacovazzo, C.; Guagliardi, A.; Moliterni, A. G. C.; Polidori, G.; Spagna, R. *J. Appl. Crystallogr.* **1999**, *32*, 115–119.

(44) Sheldrick, G. M. *SHELX97*; University of Göttingen, Göttingen, Germany, 1997.

(45) Farrugia, L. J. *J. Appl. Crystallogr.* **1999**, *32*, 837–838.

(46) Burnett, M. N.; Johnson, C. K. *ORTEP-III*; Oak Ridge National Laboratory, Oak Ridge, TN, 1996.

(47) Keller, E. *SCHAKAL97*; University of Freiburg, Freiburg, Germany, 1997.